nature neuroscience



# Cytoplasmic and mitochondrial protein translation in axonal and dendritic terminal arborization

Takahiro Chihara[1,2], David Luginbuhl[1] & Liqun Luo[1]

**We identified a mutation in *Aats-gly* (also known as *gars* or *glycyl-tRNA synthetase*), the *Drosophila melanogaster* ortholog of the human *GARS* gene that is associated with Charcot-Marie-Tooth neuropathy type 2D (CMT2D), from a mosaic genetic screen. Loss of *gars* in *Drosophila* neurons preferentially affects the elaboration and stability of terminal arborization of axons and dendrites. The human and *Drosophila* genes each encode both a cytoplasmic and a mitochondrial isoform. Using additional mutants that selectively disrupt cytoplasmic or mitochondrial protein translation, we found that cytoplasmic protein translation is required for terminal arborization of both dendrites and axons during development. In contrast, disruption of mitochondrial protein translation preferentially affects the maintenance of dendritic arborization in adults. We also provide evidence that human GARS shows equivalent functions in *Drosophila*, and that CMT2D causal mutations show loss-of-function properties. Our study highlights different demands of protein translation for the development and maintenance of axons and dendrites.**

Protein translation is an essential process in all cells. In neurons, protein translation can occur near the cell body or in distal neuronal processes (local protein synthesis). In addition to its basic functions in cell proliferation, differentiation and survival, protein translation (in particular, local protein synthesis) has been implicated in many aspects of neuronal development and function, such as axon guidance, dendritic elaboration, synaptic plasticity and long-term memory formation[1–5]. Dysfunction of the machinery that regulates protein synthesis is implicated in several human neurological disorders. For example, Fragile X syndrome, an inherited mental disorder, is caused by disruption of FMR1, an mRNA binding protein that regulates mRNA translation in neurites[6]. Moreover, errors in protein translation can lead to neurodegeneration[7]. In parallel to the protein translation in the cytoplasm, the mitochondrial genome is transcribed and translated in the mitochondria. The function and regulation of mitochondria in synaptic transmission and plasticity have been investigated in numerous systems, from rat hippocampal neurons in culture[8] to *Drosophila in vivo*[9–11]. Mitochondrial dysfunction is a common feature in neurodegenerative diseases, is the cause of some inherited neuropathies[12] and is associated with aging neurons[12,13]. Because of the 'housekeeping' functions of protein synthesis, however, the relative importance of cytoplasmic and mitochondrial protein translation for different neurobiological processes *in vivo* has not been investigated.

In a mosaic forward genetic screen to identify genes that have cell-autonomous functions in dendritic and axonal development, we found a mutant that has the following phenotype: individual mutant neurons seem to have normal growth and guidance of dendritic and axonal stalks, but fail to elaborate or stabilize terminal arborization at their targets. We identified the causal gene as *gars*, the *Drosophila* ortholog of the human Charcot-Marie-Tooth type 2D disease (CMT2D)–associated gene, which encodes human GARS[14]. Charcot-Marie-Tooth disease is an inherited autosomal dominant disease that is characterized by peripheral neuropathies in the motor and sensory neurons[15]. Molecular genetic analyses of *gars* and other mutants affecting either cytoplasmic or mitochondrial protein translation showed that defects in dendritic and axonal terminal arborization during development are caused by disruption of cytoplasmic protein translation. By contrast, impairing mitochondrial protein translation more dramatically affects the maintenance of dendritic rather than axon terminals in adults. We also show that wild-type human GARS rescues the *Drosophila gars* mutant phenotypes, and that disease-causing point mutations substantially reduce the rescuing capability.

## RESULTS

### MARCM-based screen for neuronal morphogenesis mutants

*Drosophila* olfactory projection neurons serve as a good model system for studying dendritic and axonal morphogenesis. Dendrites of individual projection neurons target a single glomerulus in the antennal lobe; the first olfactory center in the *Drosophila* brain consists of about 50 glomeruli[16]. Projection neurons elaborate highly stereotyped axon terminal arborization in higher olfactory centers according to their glomerular class[17–19]. Using the mosaic analysis with a repressible cell marker (MARCM) system[20], we can generate positively labeled projection neuron clones that are homozygous for a mutation, express a gene of interest, or both at the same time in an otherwise unlabeled and largely heterozygous animal (**Fig. 1**). This allows us to manipulate genotypes and gene expression in single or few projection neurons without affecting other cells. Furthermore, dendritic and axonal

[1]Howard Hughes Medical Institute, Department of Biological Sciences, 385 Serra Mall, Stanford University, Stanford, California 94305, USA. [2]Department of Genetics, Graduate School of Pharmaceutical Sciences, University of Tokyo, 7-3-1 Hongo, Bunkyo-ku, Tokyo 113-0033, Japan. Correspondence should be addressed to L.L. (lluo@stanford.edu).

Received 26 March; accepted 18 April; published online 27 May 2007; doi:10.1038/nn1910

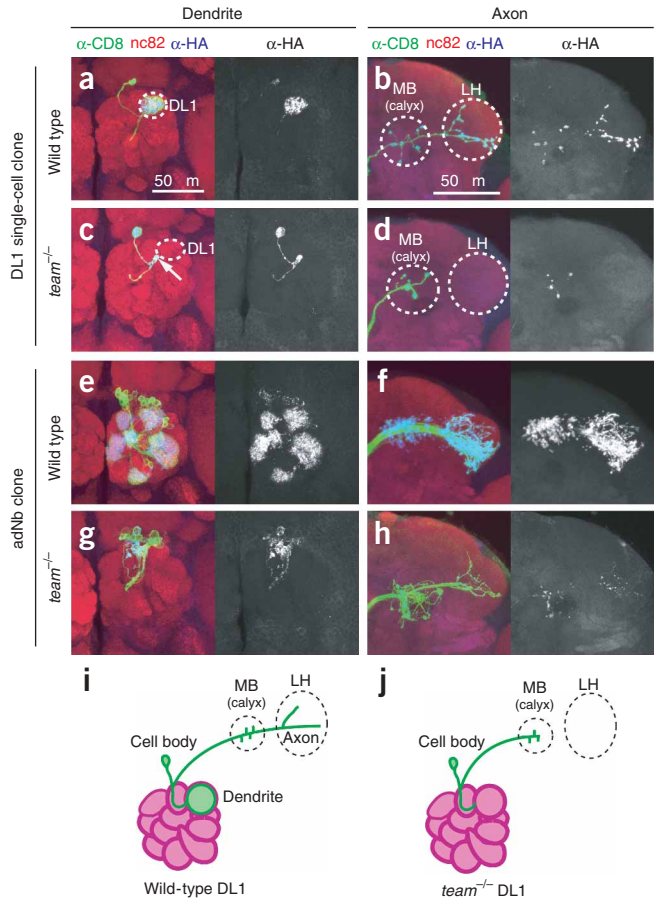


**Figure 1** Projection neurons homozygous for *team* have severely reduced dendritic and axonal terminal arborization. (**a**–**h**) Representative dendritic and axonal morphologies of projection neuron MARCM clones for wild type (**a**,**b**,**e**,**f**) and *team* mutant (**c**,**d**,**g**,**h**), labeled by mouse CD8-GFP (for projection neuron morphology in green) and syn-HA (for presynaptic terminals in blue); antibody staining for nc82, a general synaptic marker, is shown in red. Projection neuron dendrites in the antennal lobe are shown in **a**, **c**, **e** and **g**; Projection neuron axon terminals are shown in **b**, **d**, **f** and **h** in the mushroom body (MB) calyx and the lateral horn (LH) (both are circled in **b** and **d**). Right (**a**–**h**), staining channel just for antibody to hemagglutinin (blue, left). Dotted circles in **a** and **c** denote the DL1 glomerulus, the target of single-cell projection neuron clones induced by heat-shock in this study (see **Supplementary Methods**). Arrow in **c** indicates the normal dendritic targeting to the DL1 region in single-cell *team*$^{-/-}$ clone, although no dendritic terminal arborization was observed. (**i**,**j**) Schematic summary of typical wild-type and *team*$^{-/-}$ DL1 projection neuron dendritic and axonal projections. Unless indicated otherwise, all images in this and subsequent figures are maximum intensity *z*-projections of confocal stacks; dorsal is uppermost and medial is on the left.

targeting can be examined in the same preparation, allowing us to compare mechanisms of dendritic and axonal development.

To isolate mutants that affect projection neuron dendritic and axonal morphogenesis, we carried out a MARCM-based forward genetic screen (**Supplementary Methods** online). We used the *Gal4-GH146* driver, which is expressed in 90 of an estimated 150 projection neurons, to create projection neuron clones that were positively labeled and homozygous for ethylmethane sulfonate–induced mutations on the third chromosome. As reported previously[16], MARCM analysis with *Gal4-GH146* and heat shock at 4–20 h after larval hatching reproducibly generated anterodorsal projection neuron (adPN) single-cell clones of the DL1 class (with dendrites targeting to the DL1 glomerulus; **Fig. 1a**,**i**), anterodorsal neuroblast (adNb) clones (**Fig. 1e**) or lateral neuroblast clones (data not shown) with stereotyped dendritic projection patterns. DL1 single-cell clones also showed stereotypical 'L'-shape axon branching patterns in the lateral horn[17,18] (**Fig. 1b**,**i**). We took advantage of these stereotyped dendritic and axonal projection patterns of wild-type projection neurons to assess mutant dendritic and axonal phenotypes.

We screened 1,821 third chromosomes bearing ethylmethane sulfonate–induced lethal mutation(s) and found 17 mutants that show various types of dendritic and axonal morphological defects. Here, we focus on one of these mutants, *terminal arbors missing* (*team*).

### *team*$^{-/-}$ neurons have terminal arborization defects

In adult DL1 projection neuron single-cell clones homozygous for *team* (*team*$^{-/-}$), dendritic terminals were completely missing, even though dendritic stalks always extended to the vicinity of the DL1 glomerulus ($n$ = 10/10, **Fig. 1c**, arrow in left panel). Likewise, *team*$^{-/-}$ DL1 projection neuron axons often ended at the calyx region of the mushroom body with decreased numbers of synaptic buttons in the mushroom body calyx, and did not reach the lateral horn ($n$ = 7/10, **Fig. 1d**). Even in the cases when the axons did reach the lateral horn ($n$ = 3/10), the axonal terminals were much less branched than those of the wild type (**Supplementary Fig. 1** online).

Expression of a hemagglutinin-tagged synaptic vesicle protein, synaptotagmin-hemagglutinin (syt-HA)[21], made it possible to distinguish presynaptic regions of projection neuron dendrites in the glomeruli and axonal terminals in the mushroom body calyx and the lateral horn from nonsynaptic stalks that connect cell bodies to dendritic and axonal terminals (**Fig. 1a**,**b**,**e**,**f**). The localization of syt-HA proteins in projection neuron dendritic terminals in the glomeruli is consistent with the observation that, like mammalian mitral cells, projection neuron dendrites within glomeruli not only receive input from ORNs, but also send output to local interneurons[22]. Notably, instead of localizing to dendritic terminals as in wild-type projection neurons, syt-HA in *team*$^{-/-}$ projection neurons was diffusely distributed throughout the cell body and dendritic stalk, probably as a result of a lack of the normal presynaptic terminals (**Fig. 1c**, right panel).

The preferential loss of dendritic and axonal terminal arborization in *team*$^{-/-}$ projection neurons was not restricted to the DL1 class, as the same phenotype was seen in both adNb clones (**Fig. 1g**,**h**) and lNb clones (data not shown); in the wild type, these neuroblast clones project dendrites to many glomeruli[16] (**Fig. 1e**). We also observed a significant reduction in cell number in *team*$^{-/-}$ neuroblast clones (**Fig. 1e**,**g**; wild-type adNb clone: 32.6 ± 0.8 cells, $n$ = 6; *team*$^{-/-}$ adNb clone: 13.8 ± 1.9 cells, $n$ = 9; mean ± s.e.m.). As we could not determine the extent to which the defect in cell number seen in *team*$^{-/-}$ neuroblast clones contributed to terminal arborization defects, hereafter we primarily analyzed single-cell clones to focus on its postmitotic function.

In summary, a marked feature of the *team* mutant phenotype is the strong effect on terminal arborization of axons and dendrites with otherwise largely normal growth and guidance of axonal and dendritic stalks.

### *team* maps to the *glycyl-tRNA synthetase* (gars) gene

To determine the molecular basis of *team*$^{-/-}$ projection neuron clonal phenotypes, we mapped the mutation responsible for the defects (**Fig. 2**). By using a series of genetic mapping methods[23,24] (**Supplementary Methods**), we found a cytosine-to-thymine transition in *CG6778*, corresponding to the *Drosophila gars* gene (**Fig. 2a**). This

missense mutation caused an amino acid change (P98L) in the predicted catalytic domain of GARS that is conserved from yeast to human[25]. Notably, several missense mutations in the human ortholog of *gars* cause autosomal dominant CMT2D[14], which is also diagnosed as distal spinal muscular atrophy type V.

Aminoacyl-tRNA synthetases (ARSs) catalyze tRNA aminoacylation, a critical step in protein translation. Each ARS conjugates a cognate amino acid onto corresponding tRNAs (aminoacylation). In the case of GARS, it recognizes glycine and $tRNA^{gly}$ and synthesizes aminoacylated glycyl-tRNA, $Gly\text{-}tRNA^{gly}$ (ref. 26).

Two lines of evidence indicate that the missense mutation in *gars* causes the $team^{-/-}$ phenotype. First, we created a null allele of *gars* ($gars^{EX34}$) by an imprecise excision of a P element (*EY09021*) inserted in the 5′ UTR of *gars*, which removed two-thirds of the open reading frame (**Fig. 2a**). We found that projection neuron clones homozygous for $gars^{EX34}$ had phenotypes identical to that of $team^{-/-}$ projection neuron clones. These included the lack of dendritic and axonal terminal arborization in DL1 $gars^{EX34/EX34}$ single-cell clones (**Fig. 2d,e**) and reduced projection neuron cell numbers in $gars^{EX34/EX34}$ neuroblast clones (10.5 ± 1.2 cells in adNb clone, $n = 12$; mean ± s.e.m.). Second, we generated a UAS–full-length *gars* transgene (full–*gars-myc*; **Fig. 2b**) and carried out MARCM rescue experiments. In these experiments, we created $team^{-/-}$ projection neuron clones and at the same time expressed a full-length *gars* cDNA as a transgene only in labeled $team^{-/-}$ projection neurons. Transgenic expression of the full-length *gars* transgene completely rescued the $team^{-/-}$ phenotype of DL1 projection neurons ($n > 30$; **Fig. 2f,g**). It also rescued all phenotypes in $team^{-/-}$ neuroblast clones, including the defects in cell number as well as in dendritic and axonal terminal arborization ($n > 30$, data not shown). The phenotype of $gars^{EX34/EX34}$ projection neurons was also completely rescued by expression of the full-length *gars* transgene ($n > 30$, data not shown). These results demonstrate that GARS is cell-autonomously required for dendritic and axonal terminal arborization. Thus, we renamed the *team* allele as $gars^{team}$.

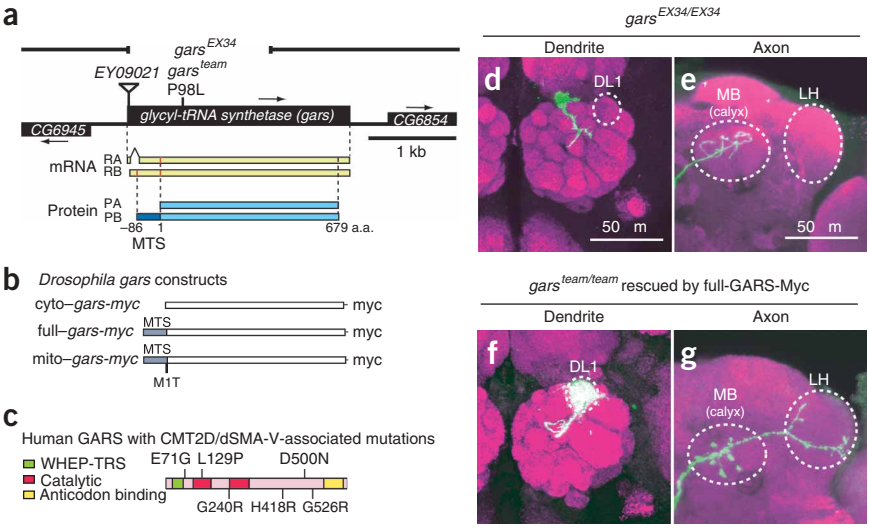


**Figure 2** Mutations in *gars* cause the *team* phenotype. (**a**) Genomic organization of the *Drosophila gars* gene. Two isoforms of *gars* mRNA (RA and RB) and protein (PA and PB) are shown in yellow and blue, respectively. Red lines in mRNA are the potential start sites for protein translation. Note that only isoform B contains the MTS at its 5′ end. The position of the *team* point mutation (P98L) is indicated on the *gars* gene structure. *EY09021*, a P-element insertion, was used for the generation of $gars^{EX34}$, a molecular null allele of *gars* gene lacking about two-thirds of *gars* ORF. (**b**) Schematic drawings of the UAS-transgenes used in this study. (**c**) Functional domains of human GARS and the positions of CMT2D-associated mutations. WHEP-TRS (green) is a helical tRNA-binding domain. (**d**–**g**) The P98L mutation in the *Drosophila gars* gene is responsible for the *team* projection neuron phenotypes. $gars^{EX34/EX34}$ DL1 projection neuron MARCM clones (**d** and **e**, mouse CD8-GFP in green) showed similar phenotypes as those of $gars^{team/team}$ DL1 projection neuron MARCM clones (**Fig. 1c,d**). The dendritic and axonal phenotypes seen in $gars^{team/team}$ MARCM clones (**Fig. 1c,d**) were completely rescued by full–*gars* transgene expression either in adPN single-cell clones (**f**,**g**) or in adNb clones (data not shown). Staining with nc82 antibody is shown in magenta.

## *gars* is required for the stability of dendritic terminals

The adult phenotypes of *gars* mutants could be caused by failure of initial elaboration of dendritic and axonal terminals, failure to stabilize these terminals after initial elaboration or a combination of both. During early pupal stages, projection neuron dendrites elaborate and target to appropriate positions in the proto-antennal lobe before the arrival of ORN axons[27]. Projection neuron dendrites first elaborate around 0 h after puparium formation (APF), and they occupy appropriate positions by 18 h APF (**Fig. 3a**). At that time, projection neuron axons have already passed the mushroom body calyx and start to innervate the lateral horn (**Fig. 3b**). At 50 h APF, although the size of the antennal lobe is smaller than that of an adult, projection neuron dendritic and axonal patterning and the formation of glomerular structures are almost complete[27] (**Fig. 3c,d**).

To determine whether the lack of dendritic and axonal terminal arborization seen in adult projection neurons is the consequence of defects in initial elaboration or stability of initially elaborated neurites, we analyzed the developing $gars^{EX34}$ projection neuron clones (**Fig. 3e–j**). At 18 h APF, DL1 single-cell $gars^{EX34}$ clones elaborate dendritic terminals similar to those of wild type in the appropriate position of proto-antennal lobe and have axonal growth that is only slightly shorter than that of wild type (**Fig. 3e,f,i,j**). However, the dendritic arborization seen at 18 h APF had completely disappeared by 50 h APF; axonal terminals have not extended beyond that seen at 18 h APF (**Fig. 3g–j**). These data suggest that axonal phenotypes may reflect a requirement of GARS for the initial elaboration in combination with subsequent stabilization, whereas the dendritic phenotype is largely caused by failure to stabilize initial dendritic terminal arborization.

## *gars* encodes both cytoplasmic and mitochondrial GARS

Protein translation is carried out in parallel in the cytoplasm and the mitochondria. In general, two ARSs corresponding to a particular amino acid are encoded by two separate genes in the nuclear genome: one for cytoplasmic and one for mitochondrial tRNA aminoacylation[26]. GARS is an exception. In yeast, both cytoplasmic and mitochondrial GARS are encoded by a single gene via alternative translational start sites[28,29]. We provide experimental evidence below that fly and human *gars* also encode both cytoplasmic and mitochondrial GARS proteins (**Fig. 4**).

A blast search in the *Drosophila* genome indicated that *CG6778* (*gars*) is the only gene encoding GARS. Furthermore, *Drosophila gars*

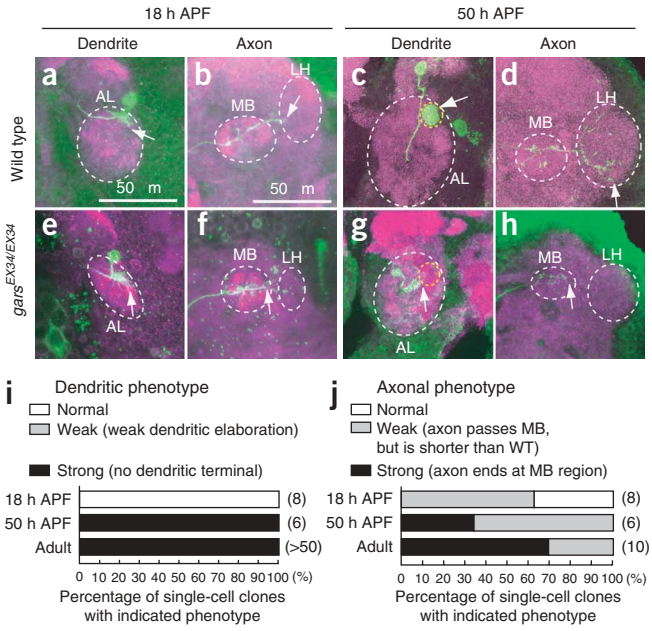


**Figure 3** Developmental studies of *gars*$^{EX34/EX34}$ phenotypes. (**a**–**h**) Representative images of developing DL1 MARCM clones (green) for wild type (**a**–**d**) and *gars*$^{EX43/Ex34}$ (**e**–**h**) at 18 h (**a**,**b**,**e**,**f**) or 50 h (**c**,**d**,**g**,**h**) APF. DN-cadherin (**a**,**b**,**e**,**f**) and nc82 (**c**,**d**,**g**,**h**) antibody stainings are shown in magenta. Dotted white circles and arrow in **a**, **c**, **e** and **g** indicate the outline of proto-antennal lobe (AL) and the tip of dendritic terminals (stalk in **g**), respectively. Dotted white circles and arrow in **b**, **d**, **f** and **h** indicate the outlines of projection neuron axonal targets (MB calyx and LH) and the tip of projection neuron axons. Dotted yellow circle in **c** and **g** indicate the position corresponding to the DL1 glomerulus in adult. At 18 h APF, projection neuron dendrites of wild-type and *gars*$^{EX34}$ projection neuron clones projected to the appropriate position in the AL (upper right portion of AL in **a** and **e**). At 50 h APF, dendritic terminals in *gars*$^{EX34}$ projection neuron clone had completely disappeared (**g**). (**i**,**j**) Quantification of dendritic (**i**) and axonal (**j**) phenotypes. Right, numbers of MARCM clones examined. Wild-type clones are essentially 100% normal.

has a potential mitochondrial targeting sequence (MTS) at the 5′ end of the open reading frame (ORF) flanked by two potential translational start sites (**Fig. 2a**). As determined by EST analysis, the *Drosophila gars* gene is predicted to have two mRNA isoforms, named as RA and RB in flybase (http://flybase.bio.indiana.edu/). RA does not contain the first translational start site and therefore lacks the MTS, whereas RB contains both potential translational start sites and the MTS (**Fig. 2a**). To determine the subcellular localization of the *Drosophila* GARS protein and the relationships of the organization of the *gars* gene, we expressed either full–*gars-myc* (full-length *gars* cDNA C-terminally tagged with an epitope), cyto–*gars-myc* (no MTS) or mito–*gars-myc* (full-length *gars-myc* with M1T missense mutation) transgenes (**Fig. 2b**) in a small subset of projection neurons, by using the *Gal4-Mz19* driver (**Fig. 4i**), and also in Cos7 cells. The M1T missense mutation in mito–*gars-myc* prevents translational initiation from the second potential translation initiator methionine as predicted by an analogous mutation in yeast[29]. As we expected, in both projection neurons and Cos7 cells, mito–GARS-Myc was colocalized with a mitochondrial marker (**Fig. 4c**,**d**), whereas cyto–GARS-Myc was distributed throughout the cytoplasm (**Fig. 4e**,**f**). Notably, full–GARS-Myc was also preferentially localized to mitochondria as much as mito–GARS-Myc (**Fig. 4a**,**b**,**g**,**h**), suggesting that the second translational initiator methionine may not be used efficiently as a translational start site in mRNA isoform RB. In summary, the *Drosophila gars* gene encodes both cytoplasmic and mitochondrial GARS, which are preferentially derived from RA and RB mRNA isoforms, respectively.

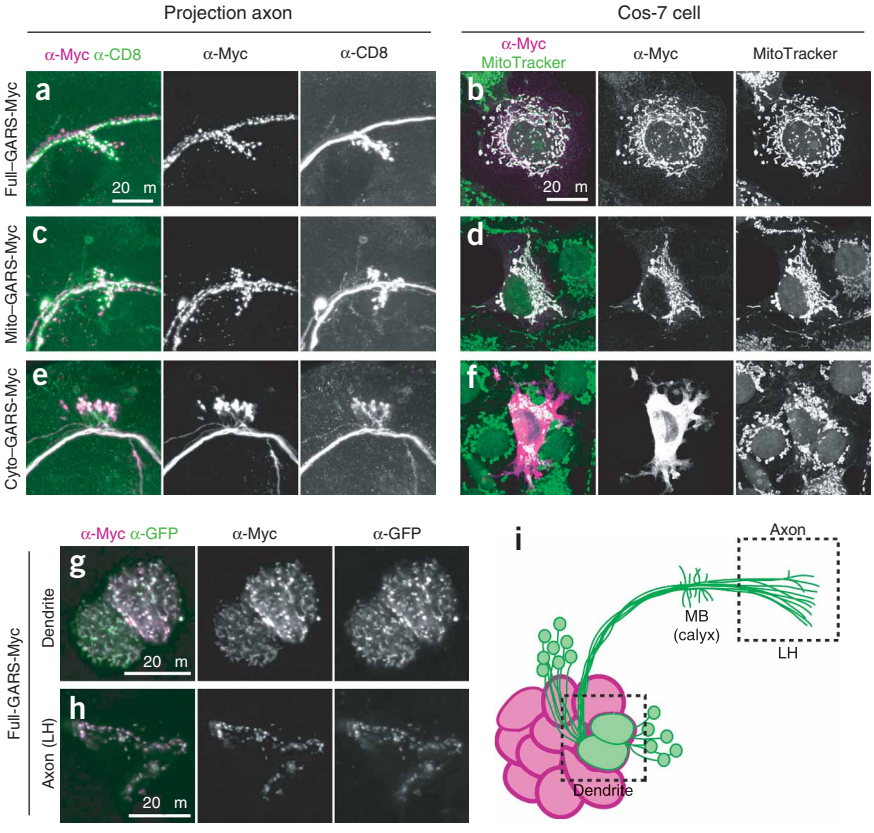


**Figure 4** *Drosophila* GARS localizes to the cytoplasm and mitochondria in projection neurons and Cos-7 cells. (**a**–**f**) Subcellular localizations of full–GARS-Myc (**a**,**b**), mito–GARS-Myc (**c**,**d**) and cyto–GARS-Myc (**e**,**f**) in projection neuron axons (**a**,**c**,**e**) and Cos-7 cells (**b**,**d**,**f**). GARS-Myc (magenta) was expressed in a subset of projection neurons by the *Gal4-Mz19* driver together with mCD8-GFP (green, labels the axon membrane) (**a**,**c**,**e**). Mitochondria in Cos-7 cells were labeled by MitoTracker (green in **b**, **d** and **f**). (**g**,**h**) Full–GARS-Myc was expressed by *Gal4-Mz19* and visualized by staining for Myc (magenta). A transgene that expressed mitochondria-targeted GFP (MitoGFP) was driven by *Gal4-Mz19* and is shown in green. Middle and right panels of **a**–**h** are images of a single channel for indicated stainings. Full–GARS-Myc and mito–GARS-Myc colocalized with mitochondrial markers (MitoTracker and Mito-GFP) in Cos-7 cells (**b**,**d**) and projection neurons (**g**,**h**), whereas cyto–GARS-Myc localized throughout the cytoplasm without specific organelle localization (**e**,**f**). (**i**) Schematic diagram of *Gal4-Mz19* expressing projection neurons. Dotted squares indicate the relative positions of dendrites and axons shown in **g** and **h**, respectively.

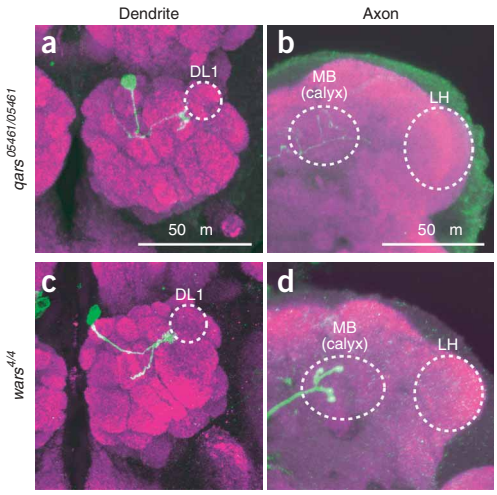


**Figure 5** Cytoplasmic protein translation is required for the dendritic and axonal terminal arborization during development. (**a**–**d**) Representative phenotypes of MARCM clones (labeled in green) are shown for cytoplasmic protein translation mutants, *qars*$^{05461}$ (**a**,**b**) and *wars*$^{4}$ (**c**,**d**). No dendritic or axonal terminal arborization was observed ($n = 10/10$ for *qars*$^{05461}$, $n = 9/9$ for *wars*$^{4}$). nc82 antibody staining is shown in magenta. The DL1 glomerulus, MB calyx and LH are outlined.

### Analysis of cytoplasmic protein translation requirement

We then sought to determine whether the dendritic and axonal terminal arborization phenotypes were caused by defects in protein translation in the cytoplasm, in the mitochondria or in both. Transgene rescue experiments did not provide clear-cut answers (**Supplementary Fig. 2** online). We therefore investigated this problem by genetically perturbing machineries that are dedicated only to either cytoplasmic or mitochondrial protein translation.

We first analyzed projection neuron clones for mutants corresponding to genes that encode only cytoplasmic ARSs. We used mutants for cytoplasmic *Aats-trp* (also known as *wars* or *tryptophanyl-tRNA synthetase*)[30] and cytoplasmic *Aats-gln* (also known as *qars* or *glutaminyl-tRNA synthetase*). These tRNA synthetases have separate genes encoding cytoplasmic and mitochondrial forms, and these mutants have intact genes encoding the corresponding mitochondrial forms. Projection neuron MARCM clones for either *wars*$^{4}$ or *qars*$^{05461}$ mutants had phenotypes that were almost identical to those of *gars* mutants. We observed markedly reduced dendritic and axonal terminal arborization in single-cell or neuroblast clones for both mutants, along with a marked reduction of cell number in neuroblast clones (**Fig. 5a–d** and data not shown). These results indicate that cytoplasmic protein translation is essential for the elaboration of dendritic and axonal terminal arborization during development.

### Analysis of mitochondrial protein translation requirement

We also examined the contribution of mitochondrial protein translation in dendritic and axonal terminal arborization by analyzing projection neuron clonal phenotypes for mitochondrial protein translation mutants (**Fig. 6**). We used *tko*$^{3}$, a null allele of *technical knockout* that encodes a mitochondrial ribosomal protein S12 (refs. 31,32). We also generated a deficiency (*Df(3L)mito*) that uncovers three genes, including two single-copy genes for mitochondrial protein translation (*mRpL12*, mitochondrial ribosome protein L12, and *CG5660*, mitochondrial valyl-tRNA synthetase) and one uncharacterized gene (*CG13313*) (**Supplementary Fig. 3** online). The projection neuron clonal phenotypes in *tko*$^{3/3}$ and *Df(3L)mito*$^{-/-}$ are very similar in both severity and penetrance (**Fig. 6g,h**). We focus below on the description of the *tko*$^{3/3}$ phenotype, which was completely rescued by a transgene that includes the *tko* genomic DNA (data not shown).

*tko*$^{3/3}$ DL1 projection neurons target their dendrites correctly to the DL1 glomerulus and have considerable elaboration (**Fig. 6c**). This is in stark contrast with *gars* or other mutants that selectively affect cytoplasmic protein translation and completely lack terminal arborization in adults (**Figs. 1** and **5**). These data support our previous conclusion that disruption of protein translation in the cytoplasm, rather than in the mitochondria, is largely responsible for the developmental defects of terminal arborization in *gars* mutants. However, we note that dendritic density in the correct glomerulus in *tko*$^{3/3}$ mutants was reduced compared with that of wild type (compare **Fig. 6a,c**; quantified in **Fig. 6g**). This phenotype became more severe with age, as in 30-d-old animals both *tko*$^{3/3}$ and *Df(3L)mito*$^{-/-}$ projection neuron dendrites no longer occupied the center of the DL1 glomerulus; instead, some dendrites surrounded the correct

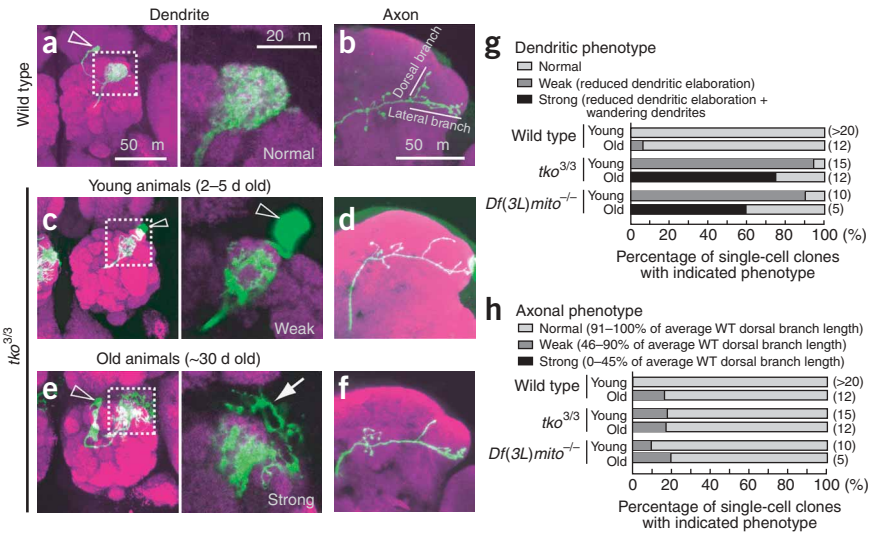


**Figure 6** Projection neuron clones defective for mitochondrial protein translation show progressive defects in dendritic, but not axonal, terminals. (**a**–**f**) Wild-type (**a**,**b**) and *tko*$^{3}$ (**c**–**f**) DL1 single-cell MARCM clones in young (**a**–**d**) and aged animals (**e**,**f**). Projection neuron clones and presynaptic regions are stained with antibody for mouse CD8-GFP (green) and nc82 antibody (magenta), respectively. Right panels of **a**, **c** and **e** are the enlarged images of the dotted squares in the left panels. Open arrowheads in **a**, **c** and **e** indicate projection neuron cell bodies. Note that dendritic terminal elaborations are sparser in the DL1 glomerulus, and are seen outside the antennal lobe in aged animals (arrow in right panel of **e**). (**g**,**h**) Quantification of dendritic (**g**) and axonal (**h**) phenotypes in projection neuron single-cell clones for wild type, *tko*$^{3}$ and *Df(3L)mito*. Representative images of each category (normal, weak and strong) for dendritic phenotypes (**g**) are shown in right panels of **a**, **c** and **e**, respectively. Progressive phenotypes are seen in dendrites of *tko*$^{3}$ and *Df(3L)mito*, but not in wild type. DL1 axonal projections are stable even in 30-d-old animals.

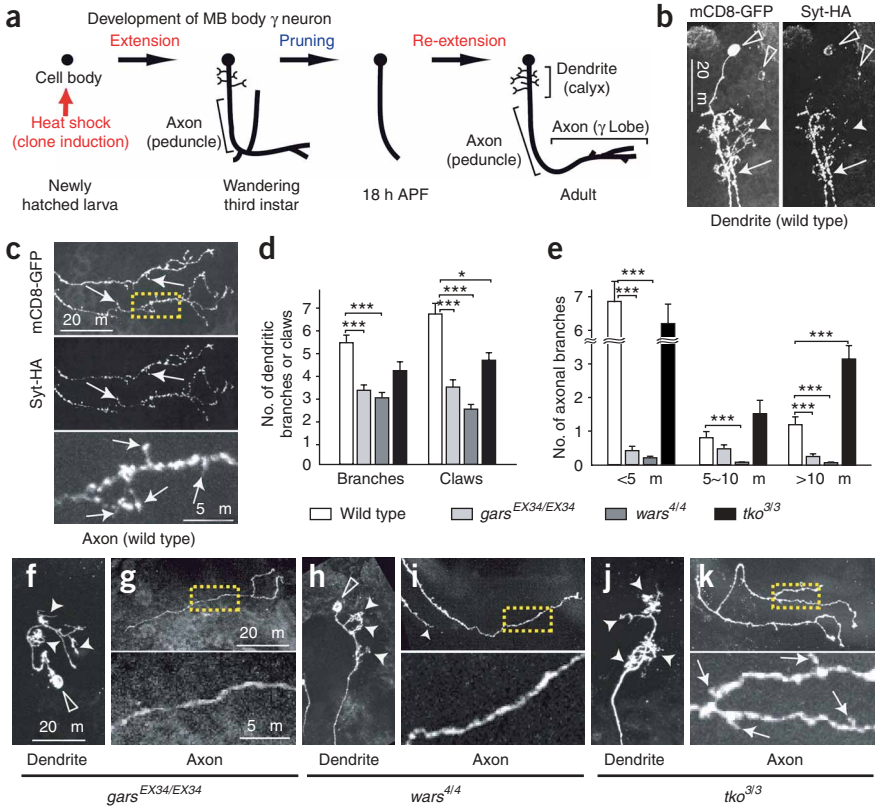


**Figure 7** Dendritic and axonal phenotypes in MB γ neurons homozygous for $gars^{EX34}$, $wars^{4}$ and $tko^{3}$. (**a**) Schematic diagram of development of MB γ neuron. (**b**,**c**) Wild-type two-cell clone of γ neuron expressing mCD8-GFP and syt-HA. Note that syt-HA localized in the axons of peduncle (arrow in **b**) and medial lobe (arrows in **c**), but not in dendritic claws (filled arrowhead in **b**). Open arrowheads denote cell bodies. (**d**,**e**) Quantitative analyses of morphological parameters of adult single-cell γ neuron clones. The numbers of clones examined were follows: wild type, $n = 14$; $gars^{EX34}$, $n = 16$; $wars^{4}$, $n = 7$; $tko^{3}$, $n = 10$ for dendritic parameters (**d**) and wild type, $n = 18$; $gars^{EX34}$, $n = 37$; $wars^{4}$, $n = 7$; $tko^{3}$, $n = 17$ for axonal parameters (**e**). Values and error bars indicate mean ± s.e.m. *, ** and *** denote $P < 0.05$, 0.01 and 0.001, respectively (two-tailed Student's *t*-test). (**f**–**k**) Representative images of single/two-cell clones of γ neuron homozygous for $gars^{EX34}$ (**f**,**g**), $wars^{4}$ (**h**,**i**) and $tko^{3}$ (**j**,**k**). Filled arrowheads in **f**, **h** and **j** indicate the position of dendritic claws. Bottom panels of **c**, **g**, **i** and **k** are enlarged images of dotted yellow squares in **c**, **g**, **i** and **k**, respectively. Arrows in bottom panels of **c** and **k** indicate many short branches in axon.

glomerulus, whereas others were outside of the antennal lobes (**Fig. 6e**; quantified in **Fig. 6g**). By comparison, the dendritic arborization of wild-type projection neuron clones in 30-d-old animals was essentially the same as in young animals (**Fig. 6g**). Analogous experiments in neuroblast clones gave qualitatively similar results (data not shown). These data indicate that mitochondrial protein translation is required for the maintenance of dendritic terminals at their correct targets, particularly during adult life.

In contrast to dendritic phenotypes, $tko^{3/3}$ and $Df(3L)mito^{-/-}$ projection neurons showed largely normal axon growth, guidance and terminal branching in single cell clones (**Fig. 6d**, compared with **Fig. 6b**) and neuroblast clones (data not shown). To determine whether subtle changes could occur, we quantified the length of the stereotyped branches in DL1 single-cell clones. In all adPN single-cell clones, either for wild type, $tko^{3}$ or $Df(3L)mito$, we did not observe obvious defects in lateral branches (wild type, $n = 20$; $tko^{3}$, $n = 20$; $Df(3L)mito$, $n = 10$; the detailed branch patterns were variable even in wild type) and found only very mild defects in the length of dorsal branches in young animals (quantified in **Fig. 6h**). This remains unchanged even in 30-d-old animals (**Fig. 6f**,**h**). These data suggest a marked difference between projection neuron axons and dendrites in their demands for mitochondrial protein translation; it is required for the maintenance of dendritic, but much less so for axonal, terminal arborization in adults.

### Protein translation requirement in mushroom body γ neurons

So far our studies have been carried out in a single neuronal type: the olfactory projection neurons that relay olfactory information from the ORNs to higher brain centers. To test the generality of our findings, we performed MARCM for essential components of protein translation in morphogenesis of another neuronal type, the mushroom body γ neurons. These neurons are involved in multimodal integration and memory[33], and their development has been well characterized[34]. During larval development, each mushroom body γ neuron extends dendrites into the calyx, and a primary axon that bifurcates into a dorsal and medial branch after passing through the peduncle (**Fig. 7a**). Shortly after puparium formation, all dendrites, as well as the dorsal and medial branches of axons, are pruned through a local degeneration mechanism[35]. Dendrites and only the medial branch of the axon begin to re-extend at 18 h APF, giving rise to the adult projection pattern. A useful feature of MARCM in adult mushroom body γ neurons is that dendrites and medial lobes are the product of re-extension during the pupal stage, which occurs about 5 d after the generation of homozygous mutant neurons, thus minimizing the perdurance of mRNA and proteins from heterozygous parental cells (**Fig. 7a**).

Each wild-type γ neuron in the adult possesses several dendritic branches in the mushroom body calyx near its cell body, and extends a single axon with several branches within the medial lobe (**Fig. 7a–c**). Dendritic branches often end in claw-like structures. There is no syt-HA staining in these dendritic claws (**Fig. 7b**, right panel), consistent with their being postsynaptic structures. Unlike projection neuron axons, in which syt-HA is concentrated in the mushroom body calyx and lateral horn, but not in the trunks (**Fig. 1**), syt-HA is distributed along the axons of mushroom body γ neurons from the peduncle to the medial lobe, and is enriched in terminal branches (**Fig. 7a**,**c**, middle panel).

We examined and quantified several morphological parameters of γ neuron single-cell clones homozygous for $gars^{EX34}$, $wars^{4}$ or $tko^{3}$ (deficient for translation in cytoplasm and mitochondria, cytoplasm alone or mitochondria alone, respectively) (**Fig. 7d–k**). We found a significant reduction in the number of dendritic branches as well as dendritic claws in mushroom body γ neurons homozygous for $gars^{EX34}$ and $wars^{4}$ (**Fig. 7f**,**h**; quantified in **Fig. 7d**). Axonal terminal branches of γ neurons were severely reduced in both mutants (**Fig. 7g**,**i**; quantified in **Fig. 7e**). Axons of $wars^{4/4}$ γ neurons often ended at the peduncle position ($n = 13/20$, arrowhead in **Fig. 7i**). In contrast to the

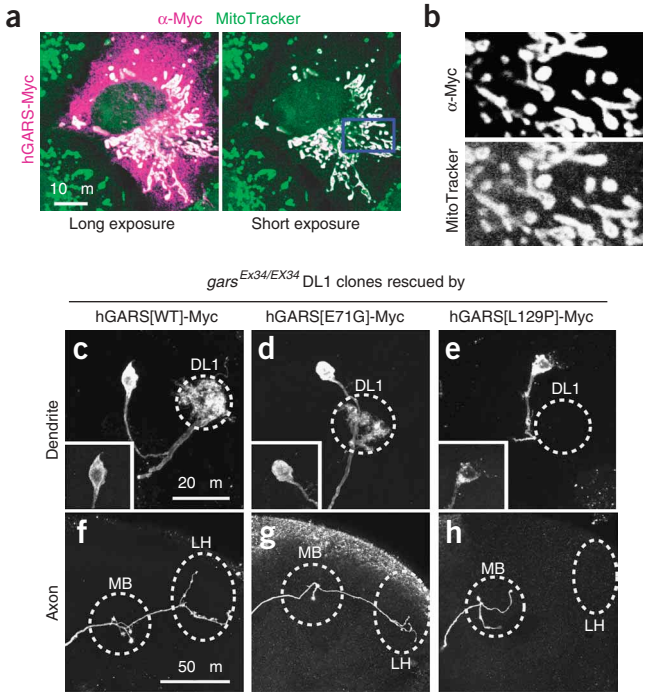


**Figure 8** Function of human GARS in *Drosophila* projection neurons. (**a**) Human GARS-MYC concentrates to the mitochondria (right panel), but is also distributed in the cytoplasm (left) in Cos-7 cells (compare with neighboring untransfected cells that are green, but not magenta). (**b**) Single channel images of hGARS-MYC (antibody to MYC, magenta in **a**) and mitochondria (MitoTracker, green in **a**) taken from blue rectangle in **a**. (**c**–**h**) MARCM-rescue experiments of $gars^{EX34/EX34}$ projection neuron clones with hGARS[WT]-Myc, hGARS[E71G]-Myc and hGARS[L129P]-Myc. DL1 glomerulus, MB calyx and LH are outlined with dotted circles. Expression levels of each transgene were monitored by staining for Myc, showing that the expression levels of all transgenes were comparable (cell body stainings with antibody for Myc are shown in insets of **c**–**e**). Dendritic and axonal arborization are fully rescued by hGARS[WT]-Myc (**c**,**f**), partially rescued by hGARS[E71G]-Myc (**d**,**g**), but not rescued at all by hGARS[L129P]-Myc (**e**,**h**).

severe defects of axon terminal branches in $gars^{EX34}$ and $wars^{4}$ mutants, γ neurons homozygous for mitochondrial translation mutant $tko^{3/3}$ had normal numbers of short (<10 μm) axonal branches (**Fig. 7e**,**k**). There was a significant increase in the number of long axonal branches (**Fig. 7e**). On the dendritic side, there was a mild reduction in the number of dendritic branches and claws in $tko^{3/3}$ mutant γ neurons, with the latter reaching statistical significance (two-tailed Student's *t*-test, $P < 0.05$, **Fig. 7d**,**j**).

Despite the differences in morphology, developmental history, synaptic distribution and circuit function, our data suggest that commonalities exist between projection neurons and mushroom body γ neurons in their sensitivity to perturbation of protein translation. Cytoplasmic protein translation affects the elaboration of dendritic and axonal terminal arborization in both mushroom body γ neurons and projection neurons. In addition, the defect in cytoplasmic protein translation can in one case ($wars^{4/4}$) interfere with the re-extension of axons as well, presumably because of more complete elimination of wild-type protein. Disruption of mitochondrial protein translation preferentially affects dendritic elaboration in both projection neuron and mushroom body γ neurons.

### Function of human CMT2D in *Drosophila* projection neurons

Several missense mutations in the human *GARS* gene cause autosomal dominant CMT2D neuropathy[14,36–38] (**Fig. 2c**). It remains to be determined whether the disease conditions are caused by gain-of-function effects of the mutant GARS or by haplo-insufficiency as a result of the loss of one copy of the gene. We wanted to distinguish between these possibilities using *Drosophila* projection neuron morphogenesis as an assay. The human *GARS* gene is predicted to encode both cytoplasmic and mitochondrial GARS proteins using alternative translation start sites. It is the only gene in the human genome that is related to *gars* found in other species, and has only a single transcript as identified by primer extension studies[39,40]. Moreover, the N terminus of human GARS is predicted to be a mitochondrial targeting sequence flanked by two potential translational start sites[25,40]. In support of this, we expressed Myc-tagged human GARS protein (hGARS-Myc) in mammalian (Cos-7) cells and found that it was concentrated in mitochondria, as well as dispersed throughout the cytoplasm (**Fig. 8a**,**b**). Thus, like that in *Drosophila*, the human *GARS* gene seems to encode both mitochondrial and cytoplasmic GARS proteins.

To investigate the possible effects of CMT2D-associated mutations in *Drosophila* projection neurons, we created transgenic flies expressing epitope-tagged wild-type human GARS and human GARS with CMT2D mutation E71G or L129P under the control of Gal4-UAS. Glu71 and Leu129 in GARS are highly conserved among yeast, fly, mouse and human (**Fig. 2c**). We first carried out overexpression experiments, in which we expressed wild-type or mutant human *GARS-MYC* genes in wild-type MARCM neuroblast and single-cell clones. We did not find morphological changes in projection neurons of young (2–5-d-old) and aged (~30-d-old) animals (data not shown).

Next, we carried out MARCM-rescue experiments, in which we expressed wild-type human *GARS-MYC* gene in $gars^{EX34/EX34}$ MARCM clones (**Fig. 8c–h**). We found that hGARS[WT]-Myc fully rescued $gars^{EX34/EX34}$ projection neuron clone phenotype including defects in dendritic and axonal arborization. DL1 single-cell clones homozygous for $gars^{EX34}$ and expressing hGARS[WT]-Myc had completely rescued dendritic and axonal arborization (**Fig. 8c**,**f**, $n = 8$). These data indicate that the roles of GARS in dendritic and axonal terminal arborization are conserved between *Drosophila* and human.

Lastly, we tested the activities of hGARS[E71G]-Myc and hGARS[L129P]-Myc for their ability to rescue $gars^{EX34/EX34}$ projection neuron clone phenotypes. We found that these two CMT2D mutations reduced the capability of hGARS to rescue $gars^{EX34/EX34}$ projection neuron clonal phenotypes to different extents. hGARS[E71G]-Myc still retained some rescue capability, although it was markedly less effective as shown by sparse dendritic elaboration (**Fig. 8d**, $n = 7$) and by the loss of the dorsal axonal branch (**Fig. 8g**, 57% of axon did not have dorsal branch. $n = 7$). hGARS[L129P]-Myc did not show any rescue capability (**Fig. 8e**,**h**), even though wild-type and mutant hGARSs were expressed at comparable levels as determined by staining with an antibody for Myc (insets of **Fig. 8c–e**). These data indicate that both CMT2D mutations have loss-of-function properties and that they affect the normal function of GARS to different degrees.

## DISCUSSION

### Role of protein translation in neurons *in vivo*

Protein translation is one of the most basic functions of all cells. The relative demand for protein translation in different aspects of neuronal morphogenesis has not been examined systematically because of its pleiotropic requirements. We perturbed cytoplasmic and mitochondrial protein translation machinery together or separately in single neurons of genetically mosaic animals. We analyzed the effect of

protein translation mutations on morphological development and the maintenance of two different types of CNS neurons with different morphology, developmental history and circuit functions. These analyses suggest that different aspects of neuronal morphogenesis *in vivo* are differentially sensitive to perturbation of protein translation.

An important caveat to the differential sensitivity interpretation is perdurance in mosaic analysis. When a projection neuron is made homozygous for *gars* via mitotic recombination, the $gars^{-/-}$ neuron inherits some wild-type *gars* mRNA and GARS protein from its parental, heterozygous cell that might compensate for the initial requirement of protein translation in mutant neurons. Earlier developmental events such as initial growth and guidance of axons and dendrites are therefore more likely to be compensated for by perdurance in *gars* homozygous neurons. We do not dispute that perdurance has a significant contribution to the differential effects we observed. Indeed, our analysis of adult mushroom body γ neuron morphogenesis showed that a subset of $wars^{-/-}$ mutant neurons also have defects in axon branch re-extension. However, the following two lines of evidence suggest that differential requirement of protein translation, in addition to perdurance, contributes to the differential phenotypes that we observed. First, loss-of-function mutations of different genes affecting cytoplasmic or mitochondrial protein translation gave rise to markedly similar and highly specific phenotypes. For instance, the projection neuron phenotypes of *gars*, *wars* and *qars* are almost identical; so are the phenotypes of *tko* and *Df(3L)mito*. These data also demonstrate that these mutant phenotypes are caused by the disruption of protein translation, rather than by noncanonical functions associated with some ARSs[41]. Second, when perdurance is minimized in our analysis of the morphogenesis of adult mushroom body γ neurons, we still find common features when compared to the morphogenesis of projection neurons. Specifically, disruption of cytoplasmic protein translation has a greater effect on dendritic and axonal terminal arborization during development than does disruption of mitochondrial protein translation. Disruption of mitochondrial protein translation preferentially affects terminal arborization of dendrites compared with axons.

Developmental analysis of *gars* mutants suggests that the lack of dendritic terminal arborization is largely caused by a failure to stabilize this arborization, rather than its initial elaboration. Whereas early elaborated dendritic terminal arborization in *gars* mutant projection neurons was completely eliminated by 50 h APF, the dendritic and axonal stalks remained largely stable even in old adults. Thus, the maintenance of terminal arborization during the period of dendritic and axonal contact and synapse formation seems to be very susceptible to perturbation of protein translation. This may reflect a higher demand for protein synthesis to support the dynamic process of synapse formation and stabilization.

We found that disruption of mitochondrial protein translation resulted in progressive defects of dendritic terminals in adults with minimal effects on axonal terminals of the same neuron. This suggests that the maintenance of dendritic terminals depends more on mitochondrial function than does that of axonal terminals. Our finding of minimal morphological abnormalities in axon terminals of mutant neurons defective for mitochondrial protein translation is consistent with several reports that analyzed mutants for axonal transport of mitochondria[9–11]. For example, *Drosophila* photoreceptor neurons homozygous for *milton* completely lack mitochondria in their axons; these neurons have severely disrupted neurotransmission, but maintain normal morphology[9]. Why are dendritic terminals more sensitive than axon terminals to perturbation of mitochondrial protein translation? One possibility is that gap junctions between mutant axons and neighboring wild-type cells alleviate some of the effects of disruptions in mitochondrial protein translation by allowing intercellular transport of metabolites, such as ATP[42]. This has been hypothesized to maintain *Drosophila* photoreceptor axons that are deprived of mitochondria because of mutations in *milton*[43]. Another possibility is that dendritic mitochondria are metabolically more active than those of axons, as has been reported in cultured embryonic rat hippocampal neurons[44]. Synaptic activity further regulates dendritic mitochondrial morphology and activity, which in turn are important for plasticity in spine and synapse morphologies[8]. Our study provides *in vivo* evidence to support the importance of mitochondrial function in the maintenance of dendritic morphology in adults.

### Implications for CMT2D neuropathy

Mutations in the human *GARS* gene cause autosomal dominant CMT2D, which is characterized by late-onset peripheral neuropathies in particular atrophies in the distal extremities. To date, six CMT2D-associated mutations in the human *GARS* gene have been found; all of them are missense mutations in conserved amino acids distributed throughout the GARS protein[14,36–38] (**Fig. 2c**). It is unclear why mutations in this essential protein result in specific phenotypes in motor neurons (and to some extent sensory neurons), and whether these mutations result in loss of function—meaning that the symptoms are caused by haplo-insufficiency—or gain of function.

Notably, a recent study showed that a spontaneous dominant mutation in the mouse *Gars* gene caused neuropathy similar to CMT2D[45]. This dominant mutation was found to be a missense mutation in the mouse *Gars* gene. Because this mutant GARS still retained normal aminoacylation activity *in vitro*, and mice heterozygous for a gene-trap loss-of-function *Gars* allele showed no phenotypes, the study concluded that there was a pathogenic role for the mutant GARS in peripheral neurons. Because this missense mutation is different from the human CMT2D mutations, these data did not directly address the nature of the human mutations.

Our results on human CMT2D mutations, E71G and L129P, are consistent with these mutations being loss-of-function alleles. First, overexpression of these mutant proteins with many different Gal4 lines did not lead to any phenotype that was detectable by examining flies grossly or at the single neuron level, even in old flies (data not shown). Second, although wild-type human GARS rescued *Drosophila gars* mutant defects in dendritic and axonal terminal arborization, human GARS with the E71G mutation rescued the phenotypes only partially, and human GARS with the L129P mutation did not rescue the phenotype at all. The different degrees of rescue may reflect the nature of the mutations: L129P maps inside the catalytic domain, but E71G maps outside it. A recent study reported that the mutation in the yeast ortholog *grs1* that is analogous to the L129P mutation led to a substantial reduction in yeast viability, consistent with our loss-of-function hypothesis, whereas yeast bearing the mutation analogous to E71G grew normally[46]. The different effect of the E71G mutation in our experiments may reflect the sensitivity of our experimental system: using the human *GARS* gene and projection neuron morphology as a readout may be sensitive enough to detect the partial loss-of-function property of the E71G mutation. Although our data do not exclude the possibility that these GARS mutants may have dominant pathogenic functions, they are at least partially loss-of-function in nature.

The loss-of-function *gars* phenotypes that we observed in *Drosophila*, including selective failure to maintain terminal arborization, are also consistent with human CMT2D mutations that selectively affect distal extremities. Why is the loss of both copies of the gene required in order for the phenotypes to be observed in *Drosophila* (we

did not find any detectable phenotypes in old flies heterozygous for $gars^{team}$ or $gars^{EX34}$, data not shown), whereas the loss of only one copy is sufficient to cause symptoms in human? This may be due to the differences in both the absolute length of axons and the lifespan of flies and humans. These differences may also account for the observation that a reduction of *gars* dose does not cause phenotypes in mice[45]. The onset of CMT2D usually occurs in teenagers, whereas the lifespan of the mouse is only ~2 years. This loss-of-function interpretation is also consistent with a recent finding that CMT2C, a different form of Charcot-Marie-Tooth disease, is caused by likely loss-of-function mutations in the human *tyrosyl-tRNA synthetase* gene[47]. Thus, the *gars* gene may be a case where different mutations cause the same disease through different mechanisms, with some acting via gain-of-function mutations[45] and others via haplo-insufficiency due to loss-of-function mutations. Our study also helped to illustrate the utility of using *Drosophila* neurons as a model system for studying human neurological disorders[48].

## METHODS

**DNA construction and generation of transgenic flies.** *gars* ORFs (full and cyto) were amplified by PCR using the *Drosophila* genome and were confirmed by sequencing. Human GARS cDNA was a gift from K. Shiba (The Cancer Institute of the Japanese Foundation of Cancer Research). Missense mutations (M1T in *Drosophila gars* gene, and CMT2D-associated mutations in human *GARS* gene) were created with the Quick Change mutagenesis kit (Stratagene). *Drosophila* and human *gars* genes with or without the appropriate mutations were subcloned into pUAST or myc-containing pUAST transformation vectors (six copies for *Drosophila* GARS-Myc, one copy for human GARS-Myc). Transgenic flies were generated using standard procedures. For human GARS-Myc expression in Cos-7 cells, we subcloned human *GARS-MYC* genes (wild type and disease mutants) into the pcDNA3 mammalian expression vector (Invitrogen). Detailed strategies of DNA constructions are available upon request.

Methods and fly stocks information used for genetic screens, mapping, immunostaining and transfection are available in the **Supplementary Methods** online.

*Note: Supplementary information is available on the Nature Neuroscience website.*


### ACKNOWLEDGMENTS

We thank R.J. Watts, E.D. Hoopfer and O. Schuldiner for contributions to mosaic genetic screening; H.T. Jocobs, D.J. Andrew, the Bloomington *Drosophila* Stock Center and the Kyoto *Drosophila* Genetic Resource Center for fly stocks; D. Berdnik, T. Komiyama, O. Schuldiner, B. Tasic and H. Zhu for comments on the manuscripts, and M. Miura for supporting T.C. to complete this work. T.C. was a recipient of a Overseas Research Fellowship from Japan Science and Technology Agency and a Postdoctoral Fellowship for Research Abroad from Japan Society for the Promotion of Science. This work was supported by US National Institutes of Health grant R01-DC005982 to L.L. and by the Sumitomo Foundation and a grant from Japan Society for the Promotion of Science to T.C. L.L. is an investigator of the Howard Hughes Medical Institute.


### AUTHOR CONTRIBUTION

T.C. designed the study with the help of L.L. T.C. conducted the experimental work and analyzed the data, D.L. assisted with the forward genetic screen, and T.C. and L.L. wrote the manuscript.

### COMPETING INTERESTS STATEMENT

The authors declare no competing financial interests.


Published online at http://www.nature.com/natureneuroscience
Reprints and permissions information is available online at http://npg.nature.com/reprintsandpermissions



1. Steward, O. & Schuman, E.M. Compartmentalized synthesis and degradation of proteins in neurons. *Neuron* **40**, 347–359 (2003).
2. Martin, K.C. Local protein synthesis during axon guidance and synaptic plasticity. *Curr. Opin. Neurobiol.* **14**, 305–310 (2004).
3. Piper, M. & Holt, C. RNA translation in axons. *Annu. Rev. Cell Dev. Biol.* **20**, 505–523 (2004).
4. Bailey, C.H., Bartsch, D. & Kandel, E.R. Toward a molecular definition of long-term memory storage. *Proc. Natl. Acad. Sci. USA* **93**, 13445–13452 (1996).
5. Horton, A.C. *et al.* Polarized secretory trafficking directs cargo for asymmetric dendrite growth and morphogenesis. *Neuron* **48**, 757–771 (2005).
6. Grossman, A.W., Aldridge, G.M., Weiler, I.J. & Greenough, W.T. Local protein synthesis and spine morphogenesis: Fragile X syndrome and beyond. *J. Neurosci.* **26**, 7151–7155 (2006).
7. Lee, J.W. *et al.* Editing-defective tRNA synthetase causes protein misfolding and neurodegeneration. *Nature* **443**, 50–55 (2006).
8. Li, Z., Okamoto, K., Hayashi, Y. & Sheng, M. The importance of dendritic mitochondria in the morphogenesis and plasticity of spines and synapses. *Cell* **119**, 873–887 (2004).
9. Stowers, R.S., Megeath, L.J., Gorska-Andrzejak, J., Meinertzhagen, I.A. & Schwarz, T.L. Axonal transport of mitochondria to synapses depends on milton, a novel *Drosophila* protein. *Neuron* **36**, 1063–1077 (2002).
10. Verstreken, P. *et al.* Synaptic mitochondria are critical for mobilization of reserve pool vesicles at *Drosophila* neuromuscular junctions. *Neuron* **47**, 365–378 (2005).
11. Guo, X. *et al.* The GTPase dMiro is required for axonal transport of mitochondria to *Drosophila* synapses. *Neuron* **47**, 379–393 (2005).
12. Chan, D.C. Mitochondria: dynamic organelles in disease, aging and development. *Cell* **125**, 1241–1252 (2006).
13. Kujoth, G.C. *et al.* Mitochondrial DNA mutations, oxidative stress and apoptosis in mammalian aging. *Science* **309**, 481–484 (2005).
14. Antonellis, A. *et al.* Glycyl tRNA synthetase mutations in Charcot-Marie-Tooth disease type 2D and distal spinal muscular atrophy type V. *Am. J. Hum. Genet.* **72**, 1293–1299 (2003).
15. Shy, M.E. Charcot-Marie-Tooth disease: an update. *Curr. Opin. Neurol.* **17**, 579–585 (2004).
16. Jefferis, G.S., Marin, E.C., Stocker, R.F. & Luo, L. Target neuron prespecification in the olfactory map of *Drosophila*. *Nature* **414**, 204–208 (2001).
17. Marin, E.C., Jefferis, G.S., Komiyama, T., Zhu, H. & Luo, L. Representation of the glomerular olfactory map in the *Drosophila* brain. *Cell* **109**, 243–255 (2002).
18. Wong, A.M., Wang, J.W. & Axel, R. Spatial representation of the glomerular map in the *Drosophila* protocerebrum. *Cell* **109**, 229–241 (2002).
19. Jefferis, G.S. *et al.* Comprehensive maps of *Drosophila* higher olfactory centers: spatially segregated fruit and pheromone representation. *Cell* **128**, 1187–1203 (2007).
20. Lee, T. & Luo, L. Mosaic analysis with a repressible cell marker for studies of gene function in neuronal morphogenesis. *Neuron* **22**, 451–461 (1999).
21. Robinson, I.M., Ranjan, R. & Schwarz, T.L. Synaptotagmins I and IV promote transmitter release independently of $Ca^{2+}$ binding in the C(2)A domain. *Nature* **418**, 336–340 (2002).
22. Ng, M. *et al.* Transmission of olfactory information between three populations of neurons in the antennal lobe of the fly. *Neuron* **36**, 463–474 (2002).
23. Berger, J. *et al.* Genetic mapping with SNP markers in *Drosophila*. *Nat. Genet.* **29**, 475–481 (2001).
24. Zhai, R.G. *et al.* Mapping *Drosophila* mutations with molecularly defined P element insertions. *Proc. Natl. Acad. Sci. USA* **100**, 10860–10865 (2003).
25. Shiba, K., Schimmel, P., Motegi, H. & Noda, T. Human glycyl-tRNA synthetase. Wide divergence of primary structure from bacterial counterpart and species-specific aminoacylation. *J. Biol. Chem.* **269**, 30049–30055 (1994).
26. Ibba, M. & Soll, D. Aminoacyl-tRNA synthesis. *Annu. Rev. Biochem.* **69**, 617–650 (2000).
27. Jefferis, G.S. *et al.* Developmental origin of wiring specificity in the olfactory system of *Drosophila*. *Development* **131**, 117–130 (2004).
28. Turner, R.J., Lovato, M. & Schimmel, P. One of two genes encoding glycyl-tRNA synthetase in *Saccharomyces cerevisiae* provides mitochondrial and cytoplasmic functions. *J. Biol. Chem.* **275**, 27681–27688 (2000).
29. Chang, K.J. & Wang, C.C. Translation initiation from a naturally occurring non-AUG codon in *Saccharomyces cerevisiae*. *J. Biol. Chem.* **279**, 13778–13785 (2004).
30. Seshaiah, P. & Andrew, D.J. WRS-85D: a tryptophanyl-tRNA synthetase expressed to high levels in the developing *Drosophila* salivary gland. *Mol. Biol. Cell* **10**, 1595–1608 (1999).
31. Royden, C.S., Pirrotta, V. & Jan, L.Y. The *tko* locus, site of a behavioral mutation in *D. melanogaster*, codes for a protein homologous to prokaryotic ribosomal protein S12. *Cell* **51**, 165–173 (1987).
32. Toivonen, J.M. *et al.* Technical knockout, a *Drosophila* model of mitochondrial deafness. *Genetics* **159**, 241–254 (2001).
33. Heisenberg, M. Mushroom body memoir: from maps to models. *Nat. Rev. Neurosci.* **4**, 266–275 (2003).
34. Lee, T., Lee, A. & Luo, L. Development of the *Drosophila* mushroom bodies: sequential generation of three distinct types of neurons from a neuroblast. *Development* **126**, 4065–4076 (1999).
35. Watts, R.J., Hoopfer, E.D. & Luo, L. Axon pruning during *Drosophila* metamorphosis: evidence for local degeneration and requirement of the ubiquitin-proteasome system. *Neuron* **38**, 871–885 (2003).
36. Sivakumar, K. *et al.* Phenotypic spectrum of disorders associated with glycyl-tRNA synthetase mutations. *Brain* **128**, 2304–2314 (2005).
37. Dubourg, O. *et al.* The G526R glycyl-tRNA synthetase gene mutation in distal hereditary motor neuropathy type V. *Neurology* **66**, 1721–1726 (2006).
38. Del Bo, R. *et al.* Coexistence of CMT-2D and distal SMA-V phenotypes in an Italian family with a GARS gene mutation. *Neurology* **66**, 752–754 (2006).

39. Bonnefond, L. *et al.* Toward the full set of human mitochondrial aminoacyl-tRNA synthetases: characterization of AspRS and TyrRS. *Biochemistry* **44**, 4805–4816 (2005).
40. Mudge, S.J. *et al.* Complex organisation of the 5′ end of the human glycine tRNA synthetase gene. *Gene* **209**, 45–50 (1998).
41. Lee, S.W., Cho, B.H., Park, S.G. & Kim, S. Aminoacyl-tRNA synthetase complexes: beyond translation. *J. Cell Sci.* **117**, 3725–3734 (2004).
42. Goldberg, G.S., Lampe, P.D. & Nicholson, B.J. Selective transfer of endogenous metabolites through gap junctions composed of different connexins. *Nat. Cell Biol.* **1**, 457–459 (1999).
43. Gorska-Andrzejak, J. *et al.* Mitochondria are redistributed in *Drosophila* photoreceptors lacking milton, a kinesin-associated protein. *J. Comp. Neurol.* **463**, 372–388 (2003).
44. Overly, C.C., Rieff, H.I. & Hollenbeck, P.J. Organelle motility and metabolism in axons versus dendrites of cultured hippocampal neurons. *J. Cell Sci.* **109**, 971–980 (1996).
45. Seburn, K.L., Nangle, L.A., Cox, G.A., Schimmel, P. & Burgess, R.W. An active dominant mutation of glycyl-tRNA synthetase causes neuropathy in a Charcot-Marie-Tooth 2D mouse model. *Neuron* **51**, 715–726 (2006).
46. Antonellis, A. *et al.* Functional analyses of glycyl-tRNA synthetase mutations suggest a key role for tRNA-charging enzymes in peripheral axons. *J. Neurosci.* **26**, 10397–10406 (2006).
47. Jordanova, A. *et al.* Disrupted function and axonal distribution of mutant tyrosyl-tRNA synthetase in dominant intermediate Charcot-Marie-Tooth neuropathy. *Nat. Genet.* **38**, 197–202 (2006).
48. Bilen, J. & Bonini, N.M. *Drosophila* as a model for human neurodegenerative disease. *Annu. Rev. Genet.* **39**, 153–171 (2005).